An Integrated Prognostics Method under Time-Varying Operating Conditions

Fuqiong Zhao, ZhigangTian[*], Eric Bechhoefer, Yong Zeng

Abstract – In this paper, we develop an integrated prognostics method considering a time-varying operating condition, which integrates physical gear models and sensor data. By taking advantage of stress analysis in finite element modeling (FEM), the degradation process governed by Paris' law can adjust itself immediately to respond to the changes of the operating condition. The capability to directly relate the load to the damage propagation is a key advantage of the proposed integrated prognostics approach over the existing data-driven methods for dealing with time-varying operating conditions. In the proposed method, uncertainties in material parameters are considered as sources responsible for randomness in the predicted failure life. The joint distribution of material parameters is updated as sensor data become available. The updated distribution better characterizes the material parameters, and reduces the uncertainty in life prediction for the specific individual unit under condition monitoring. The update process is realized via Bayesian inference. To reduce the computational effort, a polynomial chaos expansion (PCE) collocation method is applied in computing the likelihood function in the Bayesian inference and the predicted failure time distribution. Examples based on crack propagation in a spur gear tooth are given to demonstrate the effectiveness of the proposed method. In addition, the example also shows that the proposed approach is effective even when the current loading profile is different from the loading profile under which historical data were collected.

Index Terms – Integrated prognostics, time-varying operating condition, polynomial chaos expansion, Bayesian update, uncertainty quantification.

ACRONYMS AND ABBREVIATIONS

FEM   finite element modeling

PCE   polynomial chaos expansion

[*]   F. Zhao and Z. Tian are with Department of Mechanical Engineering, University of Alberta, Edmonton, AB, T6G 2G8, Canada (e-mail: ztian@ualberta.ca).

  E. Bechhoefer is with Green Power Monitoring Systems, LLC, Vermont, 05753, United States.

  Y. Zeng is with Concordia Institute for Information Systems Engineering, Concordia University, Montreal, QC, H3G 2W1, Canada.

RUL	remaining useful life
PHM	proportional hazard model
FE	finite element
SIF	stress intensity factor
MCMC	Markov chain Monte Carlo
PDF	probability density function

NOTATION

a	crack size
m, C	material parameters in Paris' law
N	number of loading cycles
ΔK	SIF range
K_I	opening mode SIF
K_{II}	sliding mode SIF
lo	loading condition
ε	model uncertainty
a^{real}	real crack size
a^{esti}	estimated crack size
a^{sim}	simulated crack size
$a_{s,N}^{sim}$	polynomial chaos approximation to simulated crack size
e	measurement error
σ	standard deviation of measurement error
ΔN	incremental number of loading cycles
$\vec{\xi}$	random vector of material parameters
$\vec{\zeta}$	Gaussian random vector with independent components
Π	joint PDF of material parameters
Σ	covariance matrix

$\boldsymbol{L}$	triangular matrix in Cholesky decomposition
ϕ	Orthogonal polynomial basis function
Φ	PDF of Gaussian random variable
X	joint PDF of independent bivariate Gaussian vector
φ	PDF of standard Gaussian random variable
Ψ	Hermite orthogonal polynomial basis function
T_{RUL}	RUL
a_0	initial crack size
a_C	critical crack size
$P_N(\cdot)$	polynomial orthogonal projection operator
$I_N(\cdot)$	function operator based on numerical integration
$f_{prior}(\cdot)$	joint prior distribution of material parameters
$l(\cdot)$	likelihood function in Bayesian inference
$f_{post}(\cdot)$	joint posterior distribution of material parameters
$\mathbb{E}(\cdot)$	expectation operator in L^2- norm

I. INTRODUCTION

Condition based maintenance (CBM) [1], [2] is a maintenance strategy based on the health condition of equipment under condition monitoring. The condition monitoring system can detect and locate anomalies through diagnostics, which provides a starting point for prognostics. The task of prognostics is to predict the remaining useful life (RUL) of the faulty component given a fault model, and expected future loading condition. Prognostics is an essential component in CBM, based on which maintenance can be scheduled in an optimal way with respect to cost, reliability, availability, or other logistic metrics of interest. Accurate, reliable prognostics methods could result in several advantages.

- Good prognostics can reduce unscheduled maintenance via providing accurate reliability information in advance.

- Asset cost can be reduced by making full use of the remaining life of critical components.

- The safety risk which operators face can be minimized via predicting the equipment health condition.

- Production can be enhanced via optimizing the maintenance policy.

- Logistic cost can be reduced by better managing spares.

Prognostics approaches can be categorized into three classes: data-driven methods [3]-[5], model-based (physics-based) methods [6]-[9], and integrated (hybrid) methods [10]-[15]. Data-driven methods rely heavily on the failure and suspension histories of the components collected from the field or laboratory, and include the proportional hazard model (PHM), and artificial intelligence based techniques [16]-[19]. They are not effective when the historical data are insufficient. Model-based methods use physical models, such as finite element (FE) models, and damage propagation models. However, it is not a trivial task to build a complex physical model with high fidelity considering all the possible interactions, and the parameters in the model are sometimes difficult to determine. Because of the limitations of both the data-driven and physics-based methods, there is a motivation for an *integrated method*, which combines the best aspects of both methods. In the integrated prognostics methods, the physical model is updated when new inspection data become available, which carry information on the health status of the component. In this way, the prediction via the model is expected to reflect the current health status, adapt itself, and predict the failure time more accurately.

The recent interest in prognostics under variable loads is fuelled by operations and maintenance personnels' need for decision support tools. Prognostics should account for changes in load, and report a more accurate RUL in a timely manner. The consideration of time-varying operating conditions in this paper is driven by the need for on-line prognostics for transportation mechanisms, manufacturing processes, numerical controlled machining, as well as other scenarios where the changes in operating conditions during operations is unavoidable. The time-varying environment could be due to the changes in temperature, load, lubrication, speed, etc. In this study, a gearbox with spur gears under varying loading condition is investigated, because loading is the most important operating condition factor for a power transmission system.

The existing studies concerning prognostics under a time-varying environment are mostly data-driven. In [20], a linear degradation model was assumed. The effects on the degradation caused by time-varying operating conditions were taken into account by the coefficients assigned to these time-varying environmental parameters. The Bayesian method was used to derive the posterior distribution of these coefficients. Because of the linear model assumption, analytical expressions for the posterior distribution as well as those for the residual life distribution were available. The authors in [21] extended the prognostics in a time-varying condition to non-linear models, in which the degradation process was assumed to be governed by a Brownian motion with linear drift. Stress changes were accounted for in the instantaneous drift parameter. Bayesian inference was employed to estimate the posterior distribution of coefficients in the drift parameter. These approaches tackle the prognostics under a time-varying condition through the coefficients estimation in the degradation model. Unfortunately, these data-driven methods do not address the physical mechanism of the degradation, and hence the load has no direct relationship with the parameters in the degradation model. In addition, the effectiveness of data-driven methods also depends heavily on the availability of a set of dense, well-distributed data. It is thus particularly challenging for a time-varying condition because it is unlikely that the training set encompasses all operating conditions.

One major challenge in prognostic algorithm development is how to capture and manage the inherent large-grain uncertainty. A number of stochastic models have been developed to investigate the uncertainty in the crack propagation process. One way to randomize the process is to hypothesize that the parameters in Paris' law are random variables, which are responsible for the scatter in failure times among identical units. Simulation methods are commonly used to quantify uncertainties in the prediction [10], [11], [14], [23]. To improve the computational efficiency, the authors' earlier work [32] discussed the application of polynomial chaos expansion (PCE) in health prognostics of a cracked gear tooth. The results showed that PCE could account for different uncertainty sources in the degradation model effectively and efficiently. The readers can refer to [24]-[31] for more details about other applications of PCE, e.g., chemical system, and fluid dynamics. In particular, PCE has its merit in dealing with the inverse problem, in which the observed measurements are used to infer system parameters. Marzouk et al. [30] proposed an efficient stochastic spectral method for the inverse problem. The idea was further developed in [33], incorporating a stochastic collocation method to tackle the

inverse problem, and a convergence proof was also given. Because the integrated prognostics process involves parameter identification in Bayesian inference, the method proposed in [33] is investigated in this present paper for a prognostics purpose.

By noticing the limitations of the existing data-driven prognostics methods, the present paper developed an integrated prognostics approach to deal with time-varying operating conditions. The degradation model is built on the physics of damage progression, which takes the form of a function of environmental parameters. Any changes of these environmental parameters, such as load, temperature, and speed, can be manifested immediately in the physical model. Hence, a key advantage of using the integrated prognostics method to deal with time-varying operating conditions is its capability to directly relate the environmental parameters to the degradation model. The proposed framework can apply to different mechanical components, given the corresponding physical models. In this study, we focus on the prognostics of a spur gear with a crack at a tooth root. The gear is a critical component in power transmission systems, and a crack is a key failure mode for gears. The well-known Paris' law [22] is applied as the damage propagation model in the theory of linear elastic fracture mechanics. A FE model for a spur gear tooth is built to calculate the stress intensity factor (SIF) at the crack tip needed in Paris' law.

Considering the uncertainty in the two correlated parameters of Paris' law, this study applies the PCE technique to improve the efficiency of the Markov Chain Monte Carlo (MCMC) algorithm when updating these uncertainties via Bayesian inference. A specific PCE formulation is given for the uncertainty quantification. By identifying the likelihood as an explicit expression of material parameters, this formulation allows a large amount of samples to ensure MCMC convergence, and enables a fast update of a joint PDF of the two correlated material parameters. Because the updated joint PDF of material parameters can better characterize the degradation process, the failure time distribution based on this joint PDF is expected to be more accurate.

The structure of the proposed approach is shown in Fig. 1. It illustrates the update process of the failure time distribution between two consecutive inspection times. This update is achieved through the update of input parameters (material parameters) in the degradation model described by Paris' law. Bayesian inference is applied to update these input parameters by taking in the condition monitoring data as observations. As this paper considers the effects of operating condition on prognostics, the loading profile is extracted to be an additional module as an input

to the FE model. The SIF is the output of the FE model, and expressed as a function with respect to crack size and load. Because this function is obtained offline by running the FE model at a baseline load and a series of selected crack sizes, there is no line connecting the data to the FE model. In this structure, Bayesian inference integrates physics models (Degradation model and FE model) and condition monitoring data (Data in Fig. 1) so that the parameters of the degradation model will become more accurate. PCE is used for two purposes: one is to calculate the likelihood function in Bayesian inference to accelerate the MCMC implementation, and the other one is to compute a failure time distribution based on the updated input parameters of a degradation model. Although a gearbox with spur gears is focused on in this paper, the proposed prognostics approach can be applied to other types of gears by using the corresponding methods and models in the SIF computation.
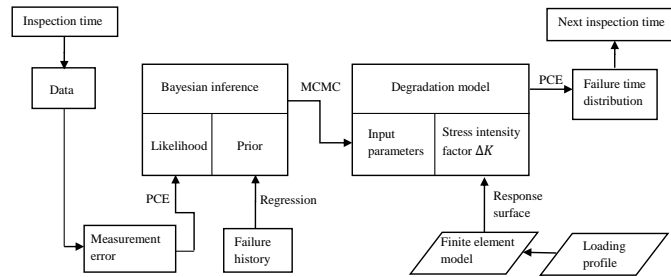

Fig. 1. Structure of the proposed prognostics approach.

This paper is organized as follows. The physical models are presented in Section II. The time-varying operating condition considered in this paper is introduced in Section III. Fundamentals of PCE for uncertainty quantification are given in Section IV. A method is proposed for material uncertainty quantification in prognostics in Section V, including a Bayesian inference framework, a specific PCE formulation to update uncertainty in two correlated material parameters, RUL prediction based on PCE, and the way to obtain the prior distributions using historical data. In Section VI, examples are given to demonstrate the effectiveness of the method. Section VII concludes the work.

II.   PHYSICAL MODELS

Compared to the existing data-driven and physics-based prognostics, the major advantages of integrated prognostics rely on the effective integration of data and degradation physics. In the case of a time-varying loading condition, the role of the physical model is particularly important because it can describe the damage propagation as a function of load. Without knowing the physics mechanism of failure, the data-driven method must train or fit to a large amount of observation data to identify a certain pattern or relationship between component health, load, and RUL, to predict the future system behavior. Obviously, data-driven prognostics need additional data sets as load condition changes over time, as any change will change the relationship already obtained during model training. In contrast, a physics-based model is established based on the physics law, which governs the material fracture under loading as well as the dynamics of the equipment. The effect of loading changes on the degradation model can be determined by stress analysis, so that the degradation model is able to adjust itself immediately after load change. In this section, two physical models needed in the present study will be introduced.

A. FE model

FE models are widely used for the stress analysis of mechanical components with complicated geometries and loading conditions. That said, analytic solutions are difficult to obtain or do not exist at all [6], [7], [9], [12], [13], [14], [23], [32]. Especially in terms of fracture problems, a discontinuity of the geometry can give rise to a singularity of the strain near the crack tip in linear elastic fracture theory. Computational fracture mechanics provides an effective way to obtain the approximate solution of the fracture problem by using the FE method and the boundary element method. SIF is an important parameter in fracture mechanics because it describes the stress filed in the region near the crack tip. Pertinent to different loading conditions that a crack can experience, as Fig. 2 illustrates, there are three types of SIF: opening mode K_I, sliding mode K_{II}, and tearing mode K_{III}. In the opening mode, the cracked body is loaded by tensile forces tending to open the crack; the sliding mode refers to in-plane shear loading, and the tearing mode corresponds to out-of-plane shear [34]. This study considers a two-dimensional problem with in-plane loading, so only K_I and K_{II} are of interest.
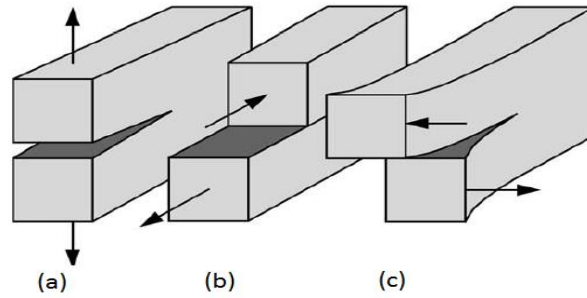
Fig. 2. Three types of loading on a cracked body:
(a) Mode I (b) Mode II (c) Mode III [34].

FE software packages facilitate the applications of the FE method in various areas, e.g., civil construction, machine design, system simulation, etc. The software FRANC2D is designed specifically for the simulation of a two-dimensional fracture process, and has been verified and used to do the analysis in many applications. FRANC2D has an appealing feature to alter the structure body geometry, and re-mesh near the crack tip automatically after the crack increments. Opening mode and sliding mode SIFs K_I and K_{II} are readily calculated using the built-in functions. In this study, FRANC2D is used to build a two-dimensional FE model for a single spur gear tooth with a crack at the root, as shown in Fig. 3. A history of SIF at different crack sizes is obtained using FRANC2D at a baseline load. Section III presents how to obtain the surface of SIF with respect to crack size and load. Because the opening mode SIF K_I dominates the crack propagation in a spur gear tooth, the SIF mentioned in the sequel refers to the opening mode SIF.
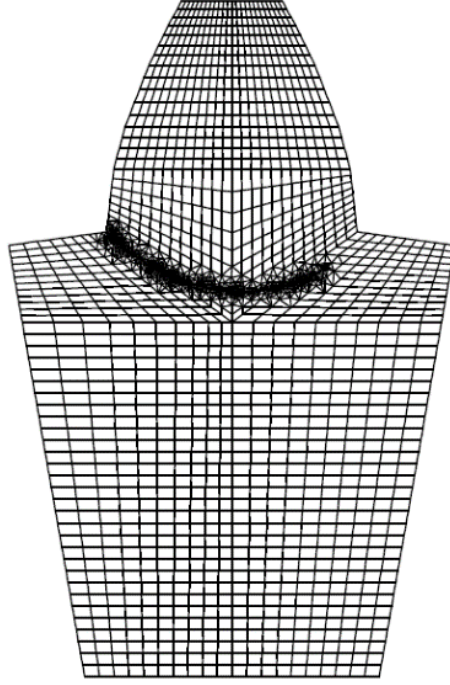
Fig. 3. A 2D FE model for a spur gear tooth [44].

B.   The degradation model

The degradation model is used for describing the damage propagation in the component over time. A failure is usually defined by the first time at which the damage indicator crosses a threshold. Most of the existing damage propagation models are built on Paris' law. Through experimental data regression, parameters in Paris' law are identified to give a fit to the degradation process. Paris' law can represent the stable stage of crack propagation after the initiation stage, and before the fast rupture stage. With the linear relationship of crack growth rate da/dN, and SIF range ΔK within one loading cycle in the log-log scale, Paris' law can be used for predicting crack propagation. For different applications, other factors apart from the range of SIF are considered in Paris' law, leading to many variants such as the Collipriest model [35], the Inoue model [36], and the Wheeler model [37]. The basic Paris' law is given by

$$\frac{\mathrm{d}a}{\mathrm{d}N} = C(\Delta K)^m. \tag{1}$$

From (1), Paris' law expresses crack growth rate $\mathrm{d}a/\mathrm{d}N$ as a function of SIF range ΔK.

Parameters C and m are material dependent parameters, experimentally estimated by fitting fatigue test data.

Fatigue crack experimental data display a large scatter in the crack size at a given cycle, as well as the number of cycles to reach a given crack size. This large scatter occurs even under a carefully controlled environment. The two material parameters C and m in Paris' law were considered as statistically correlated random variables to account for the randomness of a crack propagation process. Following the literature [11], [38], [45]-[47], in this paper, $(m, \log C)$ is assumed to obey a bivariate normal distribution. This assumption is based on fatigue experiments [38], [46], and supported by the central limit theorem [11]. Section V will include the procedure to identify the joint distribution of $(m, \log C)$ through a set of crack growth data. When a specific component with a crack comes into consideration, these material parameters should have a narrow distribution, or even a deterministic value. In this paper, the condition monitoring data on crack sizes at scheduled inspection times are used for the Bayesian inference to update the distribution of the material parameters. The distributions are expected to be narrowed down to small deviations, leading to a more accurate prediction of the RUL.

By noticing the irregularity in an individual test, the authors in [38] claimed a high frequency randomness in crack propagation. A model error ε, which is a lognormal random variable, is multiplied by the growth rate in Paris' law to account for this high frequency randomness [32]. The model error describes the quasi-random behavior of the growth law. Due to this added irregularity in the crack growth rate, the integrated crack growth curve is not a smooth function. This outcome is also shown in the Virkler data set [39]. By considering the model error ε [32], Paris' law is modified as

$$\frac{\mathrm{d}a}{\mathrm{d}N} = C(\Delta K)^m \varepsilon. \tag{2}$$

The distribution of ε can be determined by a least-square regression in a log-log scale of Paris' law using the information of crack lengths and associated cycles obtained in fatigue crack propagation experiments [40]. The residual in the regression $\zeta = \log \varepsilon$ is a zero mean Gaussian random variable. Its variance is obtained using a standard statistical method for linear regression.

When a component is subject to a time-varying loading condition, the degradation process given in (2) will depend on the load, denoted by lo. To be specific, the SIF range $\Delta K =$

$\Delta K(a, lo)$, suggesting that the model degradation rate is a function of crack size and environmental conditions. To capture the degradation pattern of a cracked component using (2), a response surface of ΔK with respect to crack size and load is needed. The following section will elaborate on how to obtain this response surface.

III. LOAD CHANGE

A piece of equipment under operation may be exposed to a series of varying loads according to the user's needs. The work logs should record two facts: the time when a loading change occurs, and the amplitude of such a change. The general case may be described as follows. Assume that totally n loading changes happen, respectively, at time $t_1, t_2 \cdots, t_n$, and that the load amplitude during $[t_i, t_j)$ is $F_{i,j}$, as shown in Fig. 4.
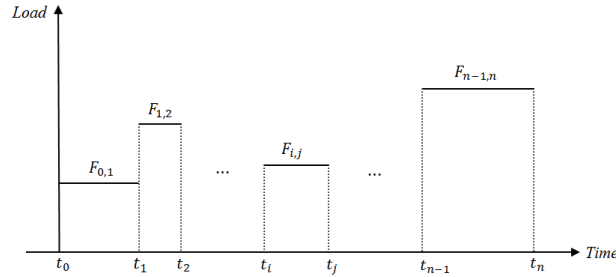

Fig. 4. General load changes history.

As discussed in the previous section, the key value that needs to be determined in the degradation model is the SIF (which determines ΔK in Paris' law), which is primarily a function of crack size, structure geometry, and loading condition. The inputs of crack size and structure geometry have already been taken into account in the FEM, while the input of loading condition is provided by the load history recorded in the work log. For complex situations, such as non-linearity and non-elasticity in the materials, the relation between ΔK and loading change needs to be obtained by running the FE analysis each time the new load is applied. In this paper, the stress analysis is constrained in the framework of linear elastic mechanics. As a result, ΔK has a linear relation with the load. By following this convention, the baseline relation of ΔK and load may be derived by running the FE model once for a baseline load only. The remaining work is merely to multiply the derived ΔK by the ratio between the new and the baseline loads. Subsequently, a surface of ΔK with respect to different crack sizes and different loads can be obtained. For

transmission systems, such as a gearbox, the load is determined by the input torque. Such an observation can significantly improve the efficiency of the proposed prognostics approach.

IV.   FUNDAMENTALS OF PCE FOR UNCERTAINTY QUANTIFICATION

Fatigue crack experimental data show a large amount of statistical scatter on the crack size at a given load, and the cycles needed to reach a given crack size. To account for the randomness in the crack propagation, the parameters in the degradation model (Paris' law in this paper) are considered as random variables so that the crack propagation process is stochastic in nature. Quantifying the uncertainty in the crack propagation process is of essential importance for equipment failure time prediction and condition based maintenance. A commonly used method to quantify the effects of input uncertainty on the output is Monte Carlo simulation. However, due to the limitations of its low convergence rate and heavy computation requirements, a more efficient, effective stochastic collocation method based on the PCE technique is applied through Bayesian inference in this paper. In this section, the fundamentals of PCE and the stochastic collocation method for uncertainty quantification are briefly presented.

Consider a model $H: \mathbf{Z} = H(\mathbf{Y})$, mapping input vector $\mathbf{Y} \in \mathbb{R}^d$ into the output $Z \in \mathbb{R}$, which is the quantity of interest. Here, for the sake of simplicity, Z is considered to be a scalar. When Z is a vector, the derived formula holds component-wise. Considering the uncertainty in the input, a probability space $(\Omega, \mathcal{F}, \mathcal{P})$ needs now to be introduced, where Ω is the event space equipped with the σ-field $\mathcal{F}$ and probability measure $\mathcal{P}$. In this space, $\mathbf{Y}$ and Z become random variables, which are functions of random event $\omega \in \Omega$. The purpose of uncertainty quantification is to study the effects of uncertainty in $\mathbf{Y}(\omega)$ on the statistical property of $Z(\omega)$. Assume that $\mathbf{Y}$ is a d-variate continuous random vector having s-independent and identically distributed (i.i.d.) components: $\mathbf{Y} = (Y_1, \cdots, Y_d)$. The joint PDF of $\mathbf{Y}$ with respect to the support $\Gamma_{\mathbf{Y}}$ is denoted as $p_{\mathbf{Y}}(\mathbf{y}) = \prod_{i=1}^{d} p_{Y_i}(y_i)$, where $p_{Y_i}(y_i)$ is the marginal PDF of Y_i.

PCE is essentially a spectral method in a probabilistic context. It relies on the fact that the unknown random response of a computational model can be approximated by the polynomials coordinated in a suitable finite orthogonal basis. Let $\boldsymbol{i} = (i_1, \cdots, i_d)$ be a multi-index with

$|\boldsymbol{i}| = i_1 + \cdots + i_d$. By using PCE, the model H can be approximated by a projection operator, $P_N: L^2 \rightarrow \mathbb{P}_N^d$, defined as

$$P_N H(\boldsymbol{Y}) = \sum_{|\boldsymbol{i}| \leq N} \hat{f}_{\boldsymbol{i}} \, \phi_{\boldsymbol{i}}(\boldsymbol{Y}) \,, \tag{3}$$

with the Fourier coefficients

$$\hat{f}_{\boldsymbol{i}} = \int_{\Gamma_Y} H(\boldsymbol{y})\phi_{\boldsymbol{i}}(\boldsymbol{y}) \, p_Y(\boldsymbol{y})d\boldsymbol{y} \,. \tag{4}$$

$\{\phi_{\boldsymbol{i}}(\boldsymbol{Y})\}_{|\boldsymbol{i}| \leq N}$ are the basis orthogonal polynomial functions in d-variate Nth-degree polynomial space $\mathbb{P}_N^d$, satisfying the orthogonality

$$\mathbb{E}[\phi_{\boldsymbol{i}}(\boldsymbol{Y})\phi_{\boldsymbol{j}}(\boldsymbol{Y})] \triangleq \int \phi_{\boldsymbol{i}}(\boldsymbol{y})\phi_{\boldsymbol{j}}(\boldsymbol{y})p_Y(\boldsymbol{y})d\boldsymbol{y} = \delta_{\boldsymbol{i}\boldsymbol{j}} \quad , 0 \leq |\boldsymbol{i}|, |\boldsymbol{j}| \leq N, \tag{5}$$

where $\delta_{\boldsymbol{i}\boldsymbol{j}}$ is d-variate Kronecker delta function. The expectation operator $\mathbb{E}$ defines an inner product in L^2 space. The series converge in the sense of the L^2-norm given that both $\boldsymbol{Y}$ and Z have finite variances is

$$\|H - P_N H\|_{L^2} \rightarrow 0, \quad N \rightarrow \infty. \tag{6}$$

The readers can refer to [31] for rigorous mathematical details of the functional space summarized above.

The selection of the basis polynomial function depends on the type of distribution of input random variables. There exists a correspondence between the basis function type and the distribution type [31]. For example, if the input random variable follows a Gaussian distribution, Hermite polynomials are selected as the basis. When the components in the input multivariable are s-independent, the multivariate basis functions can be generated in the form of products of univariate basis functions. For general cases, when s-dependence exists among the components, Soize and Ghanem did a theoretical study to clarify the associated mathematical structure of the functional space in [42]. But it may be difficult to find the orthogonal basis because of the unavailability of the joint probability density function (PDF). However, for the statistical

dependence structure in the multivariate Gaussian distribution, the correlated Gaussian random variables can be transformed into uncorrelated standard Gaussian random variables using Cholesky decomposition for the variance matrix. This method is also the approach adopted in the present paper to tackle the uncertainty in the Gaussian distributed material parameters.

With the basis functions and joint PDF available, to obtain the approximation $P_N H(\boldsymbol{Y})$ is equivalent to calculating the coefficients $\hat{f}_i$ in it. The Galerkin method, and the stochastic collocation method are two ways to obtain these coefficients. To save the effort of complex model reformulation as required by the Galerkin method, the stochastic collocation method is introduced here briefly, and used for uncertainty quantification in this paper.

The stochastic collocation method aims at estimating the coefficients in (4) by numerical integration [31]-[33], [41]. The integral in (4) is intractable when high dimensional random space is involved. In practice, the numerical integration rules provide the approximation by a weighted sum using pre-selected points $\boldsymbol{p}^{(j)} \in \mathbb{R}^d$, and the associated weights $\alpha^{(j)} \in \mathbb{R}, j = 1, \cdots, Q$, such that

$$\tilde{f}_i = \sum_{j=1}^{Q} H(\boldsymbol{p}^{(j)}) \alpha^{(j)} \to \hat{f}_i, \qquad Q \to \infty. \tag{7}$$

Various schemes can be used, which differ in the selections of the integration rules. High dimensional integration suffers from significant computation burden if employing tensor products based on a one-dimensional rule. To mitigate the computational burden, this paper utilizes a sparse grid constructed on a Smolyak algorithm [43] as the integration rule in (7).

With $\tilde{f}_i$ available, define the another operator, $I_N: L^2 \to \mathbb{P}_N^d$, such that

$$I_N H = \sum_{|i| \leq N} \tilde{f}_i \, \phi_i(\boldsymbol{Y}). \tag{8}$$

The difference between $P_N H$ and $I_N H$ is caused by the approximation of the coefficients $\tilde{f}_i \to \hat{f}_i$, and the consequent error $\|P_N H - I_N H\|_{L^2}$ is called the aliasing error. When the numerical integration rule converges, the aliasing error tends to zero, which means $I_N H$ becomes a good approximation to H.

V.   UNCERTAINTY QUANTIFICATION IN MATERIAL PARAMETERS

Manufacturing process variability may result in a difference in material at micro-structural level, such as different grain orientations. Thus, even physically identical components made of the same type of material could demonstrate different fatigue behaviors. Experimental data on crack propagation showed that, even under carefully controlled conditions, both the number of cycles taken to reach a given size, and the crack size given a number of cycles, displayed a large amount of scatter [38].

Due to its stochastic nature, the crack propagation process should be investigated from a probabilistic point of view. Paris' law is used to describe fatigue crack growth undergoing cyclic loading during its stable growth period, in which the material parameters m and C are obtained by fitting the experimental fatigue data. The variability of the crack propagation process should be reflected in the m and C statistics. It was reported in [45] that a strong correlation between m and C must be taken into consideration to achieve acceptable prediction accuracy. In practice, assume a set of experimental trajectories of stochastic crack growth is available, i.e., a set of curves representing crack growth rate da/dN vs ΔK. By linear regression using Paris' law in a log-log scale, for each trajectory, we can determine a pair of $(m, \log C)$ which minimizes the discrepancy between the measurement and the prediction. A standard statistical analysis can be applied to the sample set of $(m, \log C)$ to infer the best joint probabilistic distribution of $(m, \log C)$. It is found that the bivariate normal distribution is usually a valid hypothesis for the joint density of $(m, \log C)$ [38], [45]-[47]. The density obtained in this way can be considered as prior information; however, the values of m and C for a specific unit have very narrow distributions, or should be treated deterministically. From the perspective of condition monitoring, CBM is more concerned with fault propagation of an individual component instead of treating crack growth as a statistical property of the population. Thus, more accurate estimates of m and C for a specific unit will result in more accurate fatigue life prediction.

As discussed, precise values are often unknown for these material parameters for a specific unit. Sometimes only the prior distribution is available based on the population failure histories. In this section, considering the uncertainties in material parameters, the joint distribution of m and $\log C$ will be updated via MCMC in Bayesian inference, by taking advantage of the

condition monitoring data on crack size. As more condition data come in, the uncertainty in material parameters will be reduced, and the mean values may approach the real values.

A. Updates of the joint distribution of material parameters m and $\log C$

Considering the model error, the non-linear statistical dependence of crack growth on the loading cycle is embedded in Paris' law:

$$\frac{da}{dN} = C(\Delta K(a, lo))^m \varepsilon. \tag{9}$$

For the general case, the analytical closed-form of ΔK, as a function of crack length, loading condition, as well as structure geometry, is not available. Static FE analysis provides the discrete solution at discrete crack sizes. In this paper, a continuous form of $\Delta K(a)$ for baseline load is obtained through polynomial fitting. A surface of $\Delta K(a, lo)$ is derived by multiplying the ratio of load lo and baseline load to $\Delta K(a)$. Paris' law is a differential equation, which in nature represents a stochastic process where the material parameters behave as random processes. It is assumed that the set of material parameters $(m, \log C)$ is a random vector. Also, it was reported in [45], [46] that there exists obvious correlation between m and C. This assumption requires the joint distribution of $(m, \log C)$ to be updated given the crack sizes estimated at any given inspection time.

To solve (9), it is discretized using a first-order Euler method [48]. Let the initial crack length be a_0, and the incremental loading cycles be ΔN; then the discretized Paris' law is

$$\begin{cases} a\big((i+1)\Delta N\big) = a(i\Delta N) + (\Delta N)C[\Delta K(a(i\Delta N), lo(i\Delta N))]^m \varepsilon \\ a(0) = a_0 \end{cases}, \quad i = 0,1,2\cdots. \tag{10}$$

The iteration sequentially proceeds until the current inspection time is reached. The crack length simulated through this discretization is denoted as a^{sim}. In the simulation, model error is sampled from its assumed known distribution randomly at each iteration step.

In this study, Bayesian inference is used to update the joint distribution of m and $\log C$ at a given inspection time, given the estimated crack size at the inspection time. The real crack length is never known, but it can be estimated by using in-situ condition monitoring and diagnostics techniques. There is uncertainty in the crack length estimation, and the error between the real crack length and the estimated one is assumed to be a zero-mean Gaussian white noise with a

standard deviation of σ. The real crack size is denoted as a^{real}, and the estimated one is a^{esti}, so the measurement error is defined as $e = a^{es} - a^{real}$. Thus, $e \sim N(0, \sigma^2)$, or equivalently, $a^{esti} \sim N(a^{real}, \sigma^2)$. For a given value of $(m, \log C)$, the real crack length a^{real} at certain loading cycles is simulated by a^{sim}.

Assume that during the whole crack propagation process, from the initial detected crack a_0 to the critical crack length a_c where the failure occurs, there are totally U updates at inspection times $T_1, T_2, \cdots, T_U$. At each update time T_j, suppose that the material parameters $\vec{\xi}_j = (m_j, \log C_j)^{\mathrm{T}}$ follow a bivariate normal distribution $N(\vec{\mu}_j, \Sigma_j)$, where $\vec{\mu}_j = (\mu_{m_j}, \mu_{C_j})^{\mathrm{T}}$ is the mean vector, and Σ_j is the covariance matrix with the covariance coefficient ρ_j, where

$$\Sigma_j = \begin{bmatrix} \sigma_{m_j}^2 & \rho_j \sigma_{m_j} \sigma_{C_j} \\ \rho_j \sigma_{m_j} \sigma_{C_j} & \sigma_{C_j}^2 \end{bmatrix}. \tag{11}$$

The crack sizes $\vec{a}_{1:j} = (a_1^{esti}, a_2^{esti}, \cdots, a_j^{esti})$ at the inspection times $T_1, T_2, \cdots$ up to T_j are estimated through diagnostic methods. Then, denote the PDF of $N(\vec{\mu}_j, \Sigma_j)$ as $\Pi(\vec{\xi}_j)$,

$$\Pi(\vec{\xi}_j) = \frac{1}{(\sqrt{2\pi})^2} \frac{1}{\sqrt{\det(\Sigma_j)}} \exp\left[-\frac{1}{2} (\vec{\xi}_j - \vec{\mu}_j)^T \Sigma_j^{-1} (\vec{\xi}_j - \vec{\mu}_j) \right]. \tag{12}$$

At the next update time T_{j+1}, the crack size a_{j+1}^{esti} is estimated from sensor data. The posterior distribution of $\vec{\xi}_{j+1}$ is obtained using the Bayesian inference formula

$$f_{post}(\vec{\xi}_{j+1} | \vec{a}_{1:j+1}) = \frac{l(\vec{a}_{1:j+1} | \vec{\xi}_j) f_{prior}(\vec{\xi}_j)}{\int l(\vec{a}_{1:j+1} | \vec{\xi}_j) f_{prior}(\vec{\xi}_j) d\vec{\xi}_j}. \tag{13}$$

Given the assumption that the measurement error $e_k = a_k^{esti} - a_k^{sim}, k = 1, \cdots, j+1$ are statistically i.i.d. random variables, then the likelihood $l(\vec{a}_{1:j+1} | \vec{\xi}_j)$ is calculated as

$$l(\vec{a}_{1:j+1} | \vec{\xi}_j) = \prod_{k=1}^{j+1} \Phi_k(a_k^{esti} | \vec{\xi}_j), \tag{14}$$

where

$$\Phi_k(a_k^{esti} | \vec{\xi}_j) = \frac{1}{\sqrt{2\pi}\sigma} \exp\left[-\frac{1}{2\sigma^2} (a_k^{esti} - a_k^{sim})^2 \right]. \tag{15}$$

As time passes, new samples are collected. Accordingly, the posterior distribution of $\vec{\xi}_j = (m_j, \log C_j)^{\mathrm{T}}$ is obtained via (12) sequentially as j increases. In this way, the joint distribution of material parameters is updated to be more accurate for this specific unit under monitoring. Thus, the failure time predictions based on these parameters will be more accurate and reliable.

In the implementation of MCMC in Bayesian inference, the time-consuming part is the calculation of the likelihood function $l(\vec{a}_{1:j+1}|\vec{\xi}_j) = \prod_{k=1}^{j+1} \Phi_k(a_k^{esti}|\vec{\xi}_j)$. The Metropolis-Hastings algorithm is applied to sample the posterior distribution. For any sample $\vec{\xi}_j$ generated by a random walk, the discretized Paris' law needs to be executed to obtain the crack lengths up to the current inspection time. A large number of samples are required in simulation to ensure the posterior distribution to be the stationary state of the Markov chain. This assurance is computationally prohibitive for an on-line prognostics mission. To improve the computation efficiency, a stochastic collocation method based on a polynomial chaos technique is used, as presented in the following.

B. Polynomial chaos based stochastic collocation in Bayesian inference

In our previous work in [32], a PCE based prognostics method was proposed for efficient computation of the likelihood function in Bayesian inference when various uncertainty sources were considered to contribute to the likelihood. The specific PCE formulation was presented for updating one material parameter m in the example. This subsection presents the specific formulation of employing PCE to update two correlated material parameters m and C in Paris' law through Bayesian inference. By identifying the likelihood as an explicit expression of m and C, this formulation allows a large number of samples to ensure MCMC convergence, and enables fast update of the joint distribution of the two material parameters.

Consider the material parameters $\vec{\xi} = (m, \log C)$ in Paris' law as a random vector with two components. In this paper, $\vec{\xi}$ is assumed to follow a bivariate normal distribution with joint density function $\Pi(\vec{\xi})$, where the mean is $\vec{\mu}$, and the covariance matrix is $\mathbf{\Sigma} = \begin{bmatrix} \sigma_m^2 & \rho\sigma_m\sigma_c \\ \rho\sigma_m\sigma_c & \sigma_c^2 \end{bmatrix}$. To take advantage of the orthogonality of the basis polynomial functions to reduce the

computational work, $\vec{\xi}$ needs to be converted into a random vector $\vec{\zeta}$ whose components are standard statistically i.i.d. Gaussian variables by Cholesky decomposition,

$$\Sigma = L^T L, \tag{16}$$

$$\vec{\zeta} = L^{-1}(\vec{\xi} - \vec{\mu}). \tag{17}$$

Fig. 5, and Fig. 6 show the samples from $\vec{\xi}$, and $\vec{\zeta}$, respectively, where the correlation in $\vec{\xi}$ as well as the uncorrelated structure in $\vec{\zeta}$ are obvious to see.
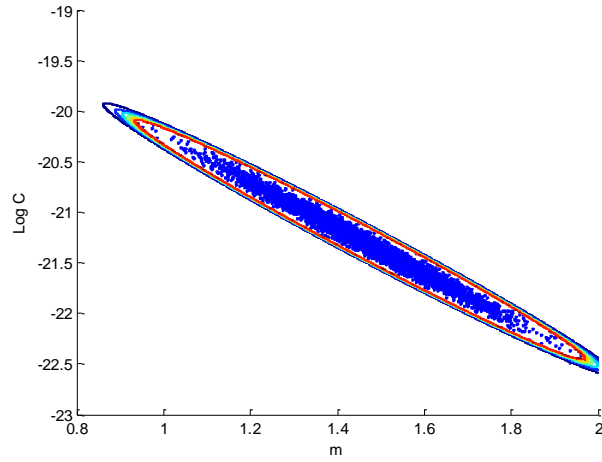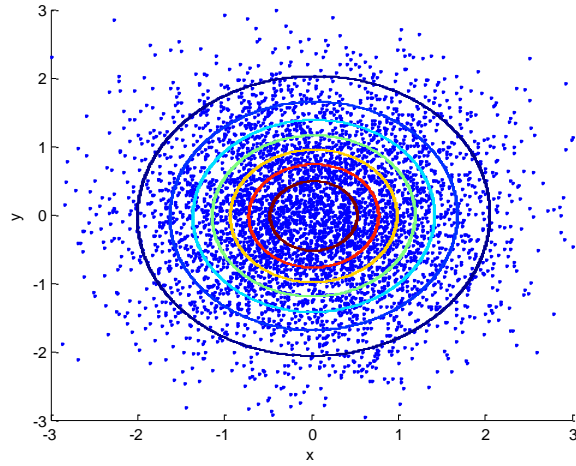
Fig. 5. Random samples from $\vec{\xi}$.

Fig. 6. Random samples from $\vec{\zeta}$.

After the change of variable, define the crack length at inspection time T obtained by Paris' law as $a^{sim}(\vec{\xi}) = a^{sim}(\vec{\mu} + L\vec{\zeta}) = a_s^{sim}(\vec{\zeta})$. The polynomial approximation to $a_s^{sim}(\vec{\zeta})$ is

20

denoted by $a_{s,N}^{sim}(\vec{\zeta})$, which is the projection in N-th order polynomial space. Following the notation in Section IV, $a_{s,N}^{sim}(\vec{\zeta}) = P_N a_s^{sim}(\vec{\zeta})$. Let $\boldsymbol{i} = (i_1, i_2)$ be an index with $|\boldsymbol{i}| = i_1 + i_2$; then,

$$a^{sim}(\vec{\xi}) = a_s^{sim}(\vec{\zeta}) \approx a_{s,N}^{sim}(\vec{\zeta}) = \sum_{|\boldsymbol{i}|=0}^{N} \widehat{w}_{\boldsymbol{i}} \, \Psi_{\boldsymbol{i}}(\vec{\zeta}). \tag{18}$$

From (4), the coefficients $\widehat{w}_{\boldsymbol{i}}$ are calculated as

$$\widehat{w}_{\boldsymbol{i}} = \mathbb{E}\left(a_s^{sim}(\vec{\zeta}) \Psi_{\boldsymbol{i}}(\vec{\zeta}) \right) = \int a_s^{sim}(\vec{\zeta}) \, \Psi_{\boldsymbol{i}}(\vec{\zeta}) \, X(\vec{\zeta}) \, d\vec{\zeta}; \tag{19}$$

and $\Psi_{\boldsymbol{i}}(\vec{\zeta})$ are the orthogonal basis functions defined as products of a one-dimensional orthogonal polynomial, satisfying, after normalization, the equality

$$\mathbb{E}\left(\Psi_h(\vec{\zeta}) \Psi_s(\vec{\zeta}) \right) = \delta_{h,s} = \begin{cases} 1, & when \ \boldsymbol{h} = \boldsymbol{s} \\ 0, & otherwise \end{cases}, \tag{20}$$

and $X(\vec{\zeta}) = \varphi(\zeta_1)\varphi(\zeta_2)$, $\varphi(x) = (1/\sqrt{2\pi})\exp(-x^2/2)$. Because the type of random vector is assumed to follow a bivariate normal distribution, a Hermite polynomial is selected as the basis function in polynomial space. To reduce computational work, a sparse grid containing R pairs of integration points and associated weights $\{(\vec{\zeta}^{(j)}, \beta^{(j)}), j = 1, \cdots, R\}$ is generated in a collocation method for computing (19) numerically as

$$\widetilde{w}_{\boldsymbol{i}} = \sum_{j=1}^{R} a_s^{sim}(\vec{\zeta}^{(j)}) \, \Psi_{\boldsymbol{i}}(\vec{\zeta}^{(j)}) \, \beta^{(j)}. \tag{21}$$

As in Section IV, define

$$I_N a_s^{sim}(\vec{\zeta}) = a_{s,I}^{sim}(\vec{\zeta}) \triangleq \sum_{|\boldsymbol{i}|=0}^{N} \widetilde{w}_{\boldsymbol{i}} \, \Psi_{\boldsymbol{i}}(\vec{\zeta}). \tag{22}$$

So, according to the PCE stochastic collocation method,

$$a_{s,I}^{sim}(\vec{\zeta}) \to a_s^{sim}(\vec{\zeta}) = a^{sim}(\vec{\xi}) \quad as \ N \to \infty, R \to \infty. \tag{23}$$

Equation (23) is of essential importance in accelerating Bayesian inference implementation because it provides an efficient way to calculate the likelihood function $l(\vec{\boldsymbol{a}}_{1:j+1}|\vec{\xi}_j) = \prod_{k=1}^{j+1} \Phi_k(a_k^{esti}|\vec{\xi}_j)$. As mentioned previously, to obtain the posterior joint distribution of

material parameters, each random walk in MCMC needs the execution of Paris' law once. A large number of MCMC samples could consume a large amount of computational time to converge. With the availability of $a_{s,I}^{sim}(\vec{\zeta})$ as an approximation to $a^{sim}(\vec{\xi})$, the expression of $a_{s,I}^{sim}(\vec{\zeta})$ is simply a combination of polynomials. For each random walk, $a^{sim}(\vec{\xi})$ is easily approximated by $a_{s,I}^{sim}(\vec{\zeta})$. The performance of such an approximation depends on the order of polynomial space as well as the number of points in the collocation set. The convergence proof can be referred to in [33].

C. Remaining useful life prediction

By using the crack size estimation as the observation, Bayesian inference is able to update the joint distribution of the material parameters. The RUL or failure time prediction is conducted after the updated distribution is available. The operation time from the current inspection cycles to the failure time is the RUL of the cracked component. Paris' law can be written in its reciprocal form as

$$\frac{\mathrm{d}N}{\mathrm{d}a} = \frac{1}{C(\Delta K(a,lo))^m \varepsilon}. \tag{24}$$

Let the current inspection cycle be N_t, and the crack increment be Δa. The RUL is calculated by discretizing (20) as

$$\Delta N_i = N_{i+1} - N_i = \Delta a [C\Delta K(a_i,lo_i)^m \varepsilon]^{-1}, i = t, t+1, \cdots \tag{25}$$

The summation $\sum_{i=t} \Delta N_i$ from the current inspection cycle to the cycle where failure occurs is the RUL. Accordingly, the total failure time is expressed as $N_t + \sum_{i=t} \Delta N_i$.

PCE is used to quantify the uncertainty of material parameters m and C in the RUL or failure time. The procedures were detailed in [32] for the case when they were considered statistically independent of each other. Here, in the presence of statistical correlation between the two material parameters, the first step is to transform these material parameters into i.i.d. random variables by using the change of variable (16) so that PCE can be applied. After this step, the remaining procedures are similar to those in [32]. The procedures are summarized here in the rest of this subsection.

Assume that an updated distribution for $\vec{\xi} = (m, \log C)$ is obtained from Bayesian inference using the method in Section V, parts A and B. After the change of variable, $\vec{\zeta} = (\zeta_1, \zeta_2)$ is a random vector with i.i.d. components, following a standard bivariate normal distribution. The density function is denoted by $X(\vec{\zeta})$, and the corresponding orthogonal basis function is $\{\Psi_i(\vec{\zeta}) \in \mathbb{P}_N^d, \ 0 \leq |i| \leq N\}$. The RUL obtained through (25) is a function of $\vec{\zeta}$, which is denoted by

$$T_{RUL} = S\left(a(\vec{\xi})\right) = T_{RUL}(\vec{\zeta}). \tag{26}$$

First, the nodal set is selected using the Smolyak algorithm, which is $\{\vec{\zeta}^{(j)}, \ j = 1, \cdots, Q\}$. Based on the proper integration rule, the associated weights $\alpha^{(j)}, j = 1, \cdots, Q$ are also available. Second, the failure times at these nodes are obtained by propagating the crack through Paris' law in a deterministic way. Denote them as $\tilde{T}^j = T_{RUL}(\vec{\zeta}^{(j)}), j = 1, \cdots, Q$. After that, we use the truncated N-th degree polynomial chaos orthogonal projection, $T_N = P_N T_{RUL}$, to approximate T_{RUL},

$$T_N = \sum_{l=1}^M \widehat{\omega}_l \Psi_l(\vec{\zeta}), \tag{27}$$

where $\widehat{\omega}_l = \int_\Gamma T_{RUL}(\vec{\zeta}) \Psi_l(\vec{\zeta}) X(\vec{\zeta}) \, d\vec{\zeta}$. Hence, (28) is valid because of (6).

$$T_N \to T_{RUL} \text{ as } M \to \infty. \tag{28}$$

Furthermore, based on (7), the coefficients $\widehat{\omega}_l$ can be approximated by $\widetilde{\omega}_l^N$ using the numerical integration rule,

$$\widetilde{\omega}_l^N = \sum_{l=1}^Q \tilde{T}^j \Psi_l(\vec{\zeta}^{(j)}) \alpha^{(j)}, \tag{29}$$

$$\widetilde{\omega}_l^N \to \widehat{\omega}_l \text{ as } Q \to \infty. \tag{30}$$

Finally, replace $\widehat{\omega}_l$ in (27) by $\widetilde{\omega}_l^N$, and we obtain

$$I_N T_{RUL} = \bar{T}_N = \sum_{l=1}^M \widetilde{\omega}_l^N \Psi_l(\vec{\zeta}), \tag{31}$$

$$\bar{T}_N \to T_N \text{ as } Q \to \infty. \tag{32}$$

$\bar{T}_N$ will converge to T_{RUL}, which is guaranteed by (28) and (32) according to the triangular inequality $\|\bar{T}_N - T_{RUL}\|_{L^2} \leq \|\bar{T}_N - T_N\|_{L^2} + \|T_N - T_{RUL}\|_{L^2}$. By increasing the number of integration nodes and the order of the polynomial space, the approximation can reach any

required accuracy. By noticing the trivial computational work needed for polynomial evaluation, and the ease of the post-processing task, PCE is an effective, efficient method to quantify the uncertainty in RUL prediction.

D. Prior distribution in Bayesian inference

To initiate the Bayesian inference, the information of the prior distribution of the material parameters is needed. Because an individual component is the focus, the population can be naturally considered as a candidate for the prior. Hence, to get the prior distribution of $(m, \log C)$, one assumes F failure histories are available for identical gear sets under identical constant loading conditions. Each history serves as a degradation path, with loading cycles and the associated crack sizes. Following the standard crack fatigue test procedure [40], the linear regression of $(m_i, \log C_i)$, $i = 1, 2, \cdots, F$, can be obtained for each failure history. Let

$$\bar{m} = \frac{1}{F} \sum_{i=1}^{F} m_i, \; s_{mm} = \frac{1}{F-1} \sum_{i=1}^{F} (m_i - \bar{m})^2, \tag{33}$$

$$\overline{\log C} = \frac{1}{F} \sum_{i=1}^{F} \log C_i, \quad s_{cc} = \frac{1}{F-1} \sum_{i=1}^{F} (\log C_i - \overline{\log C})^2, \tag{34}$$

$$s_{mc} = \frac{1}{F-1} \sum_{i=1}^{F} (m_i - \bar{m})(\log C_i - \overline{\log C}), \tag{35}$$

$$\boldsymbol{S}_{mc} = \begin{bmatrix} s_{mm} & s_{mc} \\ s_{mc} & s_{cc} \end{bmatrix}. \tag{36}$$

Then the prior distribution is selected to be $N\left([\bar{m}, \overline{\log C}]^T, \boldsymbol{S}_{mc}\right)$. The regression process can also be implemented by simulation based optimization. The readers can refer to [44] for details. The objective is to find the optimal value $(m_i^{op}, \log C_i^{op})$, $i = 1, 2, \cdots, F$, which generates the degradation path that has the minimum difference from the real degradation path in a least-square sense.

VI.   EXAMPLES

The crack propagation at the root of a spur gear is taken as an example to demonstrate the proposed method. Due to cyclic loading, the gear tooth is subject to periodic bending stress at one side, and the crack is prone to be initiated at the root where the maximum bending stress occurs. The FE model of a single tooth is built using the FE software package FRANC2D, as shown in Fig. 3. The geometry parameters and material properties are listed in Table I. The crack at the gear tooth root starts at an initial length of 0.1 mm, and the tooth is considered to be failed when the crack size reaches 5.2 mm, which is about 80% of the circular thickness of the tooth. Opening mode SIF (K_I) dominates the fracture behaviour. The baseline load for calculating ΔK is selected to be 40 N-m. The response surface of SIF as a function of crack size and load is shown in Fig. 7. According to the linear elastic model, this surface is linear in terms of load, and nonlinear with respective to crack size. Here, a cubic polynomial is used to statistically fit this nonlinearity in a least-square sense. With this surface function available, the SIF at any combination of load and crack size is obtained by simply looking up the corresponding value in this surface. Hence, it is unnecessary to run the FE analysis for every case during online prognosis, which saves considerable computational time.

Ten degradation paths are generated using the parameters $\mu_m = 1.4354$, $\mu_c = -23.118$, $\sigma_m = 0.2$, $\sigma_c = 0.5$, $\rho = -0.99$. Two examples are conducted in this section. The loading change pattern in Example 1 is a two-step stress change, where the stress is held constant during two consecutive load change points. The purpose is to demonstrate that, as more crack estimations are incorporated into Bayesian inference, the mean of the joint distribution of $(m, \log C)$ will approach their real values, and the shape of the distribution will get narrower. As a result, the uncertainty is reduced significantly. As uncertain parameters become more accurate, the predicted failure time will converge to the real failure time. Furthermore, in Example 2, we will show that the proposed method is effective even when the loading profile changes. A loading profile with a three-step stress change is used. It demonstrates that two different loading histories will result in similar narrow posterior distributions for $(m, \log C)$.
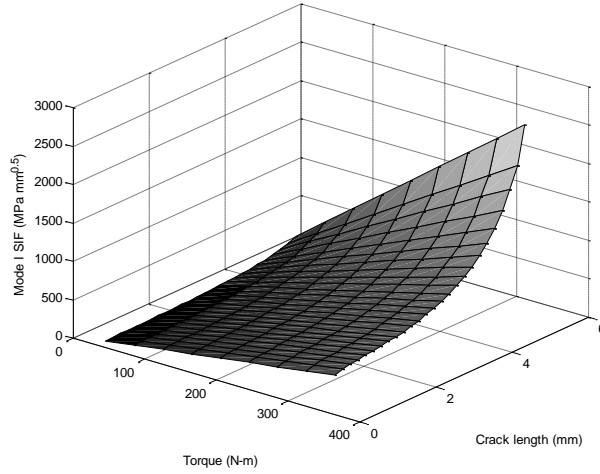
Fig. 7. Surface of SIF as function of load and crack size.

Table I

Material properties, and main geometry parameters [44]

Young's modulus (Pa)	Poisson's ratio	Module (mm)	Diametral pitch (in^{-1})	Base circle radius (mm)	Outer circle (mm)	Pressure angle (degree)	Teeth No.
2.07e11	0.30	3.20	8.00	28.34	33.30	20.00	19

A. Example 1

The simulated degradation paths with measurement error $\sigma = 0.15$ mm are shown in Fig.8. Suppose that the torque is increased from 40 N-m to 120 N-m at 0.5×10^7 cycles, and returns to 40 N-m at 2×10^7 cycles. Under this two-step load change condition, a distinct change on the slope of the crack size as a function of loading cycles is observed in Fig. 8 during the period from 0.5×10^7 cycles to 2×10^7 cycles, because the crack growth rate is increased as the torque doubles itself. The prior distribution is obtained based on the first 8 paths among these ten paths as

$$(m, \log C) \sim N\left(\begin{bmatrix} 1.4472 \\ -23.12 \end{bmatrix}, \quad \begin{bmatrix} 0.0229 & -0.052 \\ -0.052 & 0.1203 \end{bmatrix}\right).$$
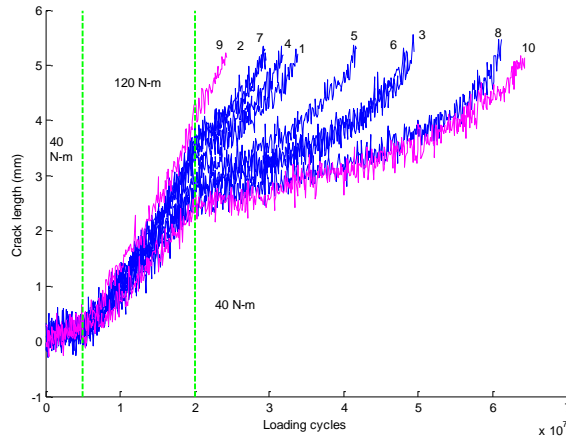
Fig. 8. Ten degradation paths generated under two-step stress changes.

To test the proposed method, two extreme paths, Path #9, and Path #10, are selected, which have the shortest failure time, and the longest, respectively. The Bayesian updating is performed at each inspection time, which is equally spaced. Some of the intermediate update steps will be tabulated in the table to show the trend of distribution adjustment as more data on crack length become available.

The real material parameters used to generate Path #9 is $(m, \log C) = (1.1495, -22.4311)$, and the real failure time is 2.43×10^7 cycles. The inspection time interval is 4×10^6 cycles. The updating results are shown in Table II, from which it can be observed that the statistical mean values of the material parameters are approaching their real values as more observations are available. Fig. 9 displays the contours of the prior and posterior distributions of the last update. The update of the failure time distribution obtained using the updated material parameters distribution is displayed in Fig. 10. The failure time distribution gets narrower, and approximates the real failure time as expected. The uncertainty in the predicted failure time is also reduced during the model parameter updating process.

Table II

Test results for path #9

Inspection cycle	Crack length (mm)	μ_m	μ_C
0	0.1000	1.4472	-23.1200
8×10^6	0.6373	1.4590	-23.1479

27

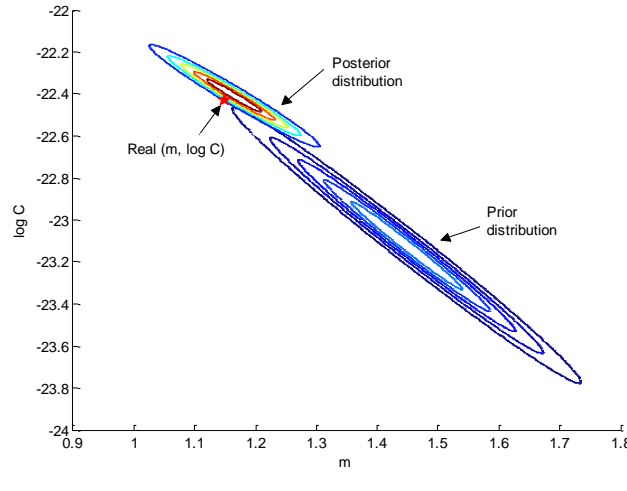| 12×10^6 | 2.2764 | 1.1871 | -22.4771 |
| 16×10^6 | 2.8742 | 1.1637 | -22.4067 |

r

Fig. 9. Contours of prior and posterior distributions of $(m, \log C)$ of path #9.
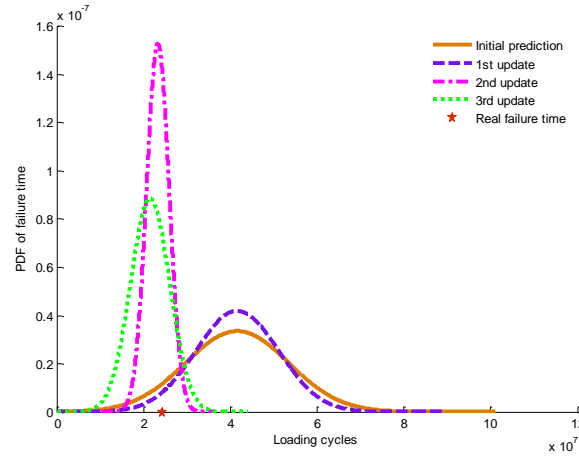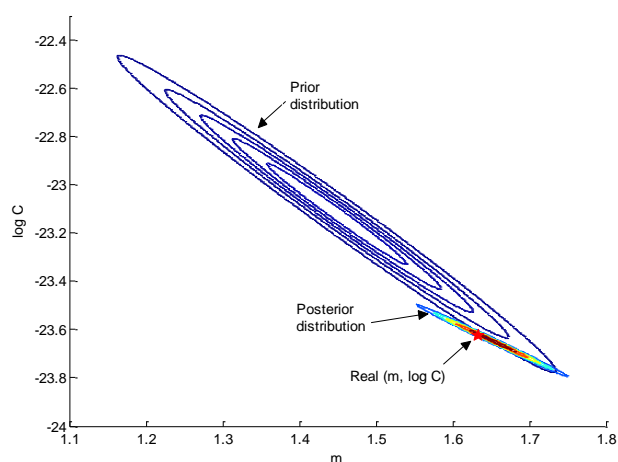

Fig. 10. Updated failure time distribution for path #9.

Similarly, the updating results for Path #10, which has the longest failure time, are shown in Table III. The real material parameters used to generate Path #10 are $(m, \log C) = (1.6336, -23.6258)$, and the real failure time is at 6.43×10^7 cycles. The inspection time interval is 10×10^6 cycles. The contours of the prior and posterior distributions of the last update are shown in Fig. 11. The predicted failure time distributions are presented in Fig. 12. The parameters adjust themselves to get close to their real values. Accordingly, the uncertainty in the failure time distribution is reduced gradually, the mean of which approaches the true failure time.

Table III

Test for path #10 to validate proposed approach

Inspection cycle	Crack length (mm)	μ_m	μ_C
0	0.1000	1.4472	-23.1200
10×10^6	0.7293	1.5670	-23.4063
20×10^6	2.4450	1.6515	-23.6117
60×10^6	4.3758	1.6510	-23.6457

Fig. 11. Contours of prior and posterior distributions of $(m, \log C)$ of path #10.
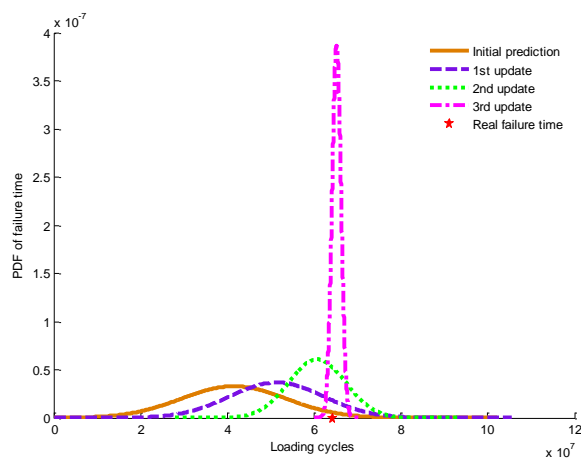

Fig. 12. Updated failure time distribution for path #10.

B.   Example 2

For a specific gear, the values of $(m, \log C)$ are material dependent, and are not supposed

to change with different loading profiles. In this example, path #11 is subject to a loading profile different from that in Example 1, and a three-step stress change is used. At 0.5×10^7 cycles, the torque increases from 40 N-m to 160 N-m; at 1.5×10^7 cycles, the torque returns to 40 N-m; and at 3×10^7 cycles, the torque goes up to 120 N-m until the component failed. The degradation path is shown in Fig. 13. The true value of this component is $(m, \log C) = (1.6336, -23.6258)$, the same as that in path #10 in Example 1. The real failure time is 3.44×10^7 cycles. The inspection time interval is 4×10^6 cycles. The statistical properties of the updated distributions as well as the crack size observations are listed in Table IV. Even though the last update of the parameters $(m, \log C)$ deviate a small amount from their real values, the failure time distribution gets closer to the real failure time at each update, shown in Fig. 14. This example demonstrates that the proposed method is effective, even when the current loading profile is different from the loading profile under which historical data were collected.

It may be worth noticing that, in Paris' law, different combinations of m and C could lead to the same crack length at a given number of loading cycles. Because the crack length is taken as the observation to update the material parameters, the Bayesian inference tries to generate distributions that maximize the occurrence of crack observations. The failure is defined by a critical crack length. When the measurement error is too large for the Bayesian inference to discriminate the real values of $(m, \log C)$ from the noise, there is a possibility that the updated $(m, \log C)$ deviates from the true value. However, the failure time still approaches the real failure time. A similar conclusion was made in [11].
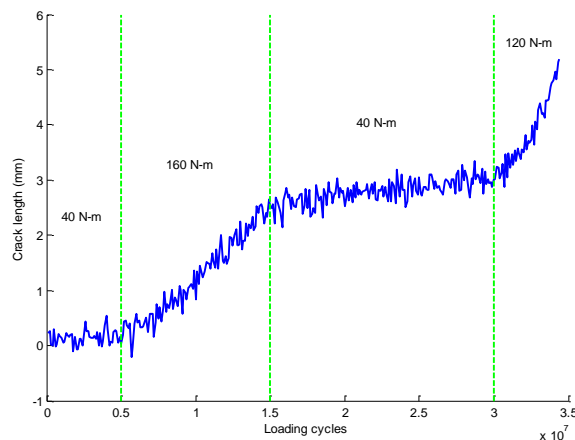
Fig. 13. Degradation path of #11 under three-step stress changes.

Table IV

Test for path #11 to validate proposed approach

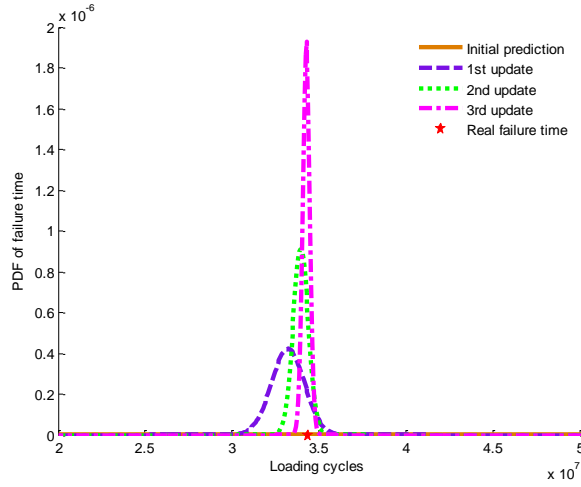| Inspection cycle	Crack length (mm)	μ_m	μ_C
0	0.1000	1.4472	-23.1200
12×10^6	1.6192	1.6036	-23.5285
20×10^6	2.5303	1.6547	-23.6579
32×10^6	3.5021	1.6972	-23.7521

Fig. 14. Updated failure time distribution for path #11.

VII.   CONCLUSIONS

An integrated prognostics method considering time-varying operating conditions is developed, which integrates physical models and sensor data from gearboxes. By taking advantage of stress analysis in finite element modeling, the degradation process governed by Paris' law can adjust itself immediately to respond to the changes of the operating condition. In the proposed method, uncertainties in material parameters are considered as sources responsible for randomness in the predicted failure life. The joint distribution of material parameters is updated as the sensor data are available. The updated distribution characterizes the material parameters, and reduces the uncertainty for the specific individual unit under monitoring. The update process is realized via Bayesian inference. To reduce the computational effort, a PCE collocation method is applied to computing the likelihood function in the Bayesian inference, and the predicted failure time distribution. An example of crack propagation at a spur gear tooth

root is given to demonstrate the effectiveness of the proposed method. Even though the gearbox is considered in this paper, the proposed method is also applicable to various other components and structures subject to the similar fatigue loading after the appropriate adjustment of physical models.

The capability to directly relate the load to the damage propagation is a key advantage of the proposed integrated prognostics approach over the existing data-driven methods for dealing with time-varying operating conditions. The proposed approach is effective even when the current loading profile is different from the load profile under which historical data were collected. Future efforts will be invested to validate the proposed approach in a lab environment.

REFERENCE

[1]   A.K.S. Jardine, D. M. Lin, and D. Banjevic, "A review on machinery diagnostics and prognostics implementing condition-based maintenance," *Mechan. Syst. Signal Process.*, vol. 20, no.7, pp. 1483-1510, 2006.

[2]   D. Banjevic, A. K. S. Jardine, V. Makis and M. Ennis, "A control-limit policy and software for condition-based maintenance optimization," *INFOR*, vol. 39, no. 1, pp. 32-50, 2001.

[3]   N. Gebraeel, M. A. Lawley, and R. Liu, "Residual life, predictions from vibration-based degradation signals: A neural network approach," *IEEE Trans. Ind. Electron.*, vol. 51, no. 3, pp. 694-700, 2004.

[4]   N. Gebraeel and M. A. Lawley, "A neural network degradation model for computing and updating residual life distributions," *IEEE Trans. Autom. Sci. Eng.*, vol. 5, no. 1, pp. 154-163, 2008.

[5]   N. Gebraeel, M. Lawley, R. Li, and J. K. Ryan, "Life Distributions from Component Degradation Signals: A Bayesian Approach," *IIE Trans. Qual. Reliab. Eng.*, vol. 37, no. 6, pp. 543-557, 2005.

[6]   C. J. Li and H. Lee, "Gear fatigue crack prognosis using embedded model, gear dynamic model and fracture mechanics," *Mechan. Syst. Signal Process.*, vol. 19, no. 4, pp. 836–846, 2005.

[7]   G. J. Kacprzynski, A. Sarlashkar, M. J. Roemer, A. Hess, and G. Hardman. "Predicting remaining life by fusing the physics of failure modeling with diagnostics," *J. Minerals, Metals Mater. Soc.*, vol. 56, no. 3, pp. 29-35, 2004.

[8]   S. Marble and B. P. Morton, "Predicting the remaining life of propulsion system bearings," in *Proc. 2006 IEEE Aerospace Conf.*, Big Sky, MT, USA, 2006.

[9]   S. Glodez, M. Sraml, and J. Kramberger, "A computational model for determination of service life of gears," *Int. J. Fatigue*, vol. 24, no. 10, pp. 1013-1020, 2002.

[10] A. Coppe, R. T. Haftka, and N. H. Kim, "Uncertainty reduction of damage growth properties using structural health monitoring," *J. Aircraft*, vol. 47, no. 6, pp. 2030-2038, 2010.

[11] D. An, J. Choi, and N. H. Kim, "Identification of correlated damage parameters under noise and bias using Bayesian inference," *Struct. Health Monit.*, vol. 11, no. 3, pp. 293-303, 2012.

[12] M. E. Orchard and G. J. Vachtsevanos, "A particle filtering approach for on-line failure prognosis in a planetary carrier plate," *Int. J. Fuzzy LogicIntell. Syst.*, vol. 7, no. 4, pp. 221-227, 2007.

[13] M. E. Orchard and G. J. Vachtsevanos, "A particle filtering-based framework for real-time fault diagnosis and failure prognosis in a turbine engine," presented at the 2007 Mediterranean Conf. on Contr. Autom., Athens, Greece, 2007.

[14] S. Sankararaman, Y. Ling and S. Mahadevan, "Confidence assessment in fatigue damage prognosis," presented at the Annu. Conf. Prognos. Health Manag. Soc., Portland, OR, USA, 2010.

[15] E. Bechhoefer, A. Bernhard and D. He, "Use of Paris law for prediction of component remaining useful life," in *Pro. 2008 IEEE Aerospace Conf.*, Big Sky, MT, USA, 2008.

[16] R. B. Abernethy, *The New Weibull Handbook*. 2nd ed. Abernethy, North Palm Beach, 1996.

[17] D. R. Cox, "Regression models and life-tables", *J. Roy. Statist. Soc. Ser. B.*, vol. 34, no. 2, pp. 187-220, 1972.

[18] Z. Tian, L. Wong, and N. Safaei, "A neural network approach for remaining useful life prediction utilizing both failure and suspension histories," *Mechan. Syst. Signal Process.*, vol. 24, no. 5, pp. 1542-1555, 2010.

[19] Z. Tian and M. J. Zuo, "Health condition prediction of gears using a recurrent neural network approach," *IEEE Trans. Reliab.*, vol. 59, no. 4, pp. 700-705, Dec. 2010.

[20] N. Gebraeel and J. Pan, "Prognostic degradation models for computing and updating residual life distributions in a time-varying environment," *IEEE Trans. Reliab.*, vol. 57, no. 4, pp. 539-550, 2008.

[21] H. Liao and Z. Tian, "A framework for predicting the remaining useful life of a single unit under time-varying operating conditions*," IIE Trans.*, vol.45, no.9, pp. 964-980, 2013.

[22] P. C. Paris and F. Erdogen, "A critical analysis of crack propagation laws," *J. Basic Eng.*, vol. 85, no. 4, pp. 528-534, 1963.

[23] S. Sankararaman, Y. Ling, S. Mahadevan, "Uncertainty quantification and model validation for fatigue crack growth prediction," *Eng. Fract. Mech.,* vol.78, pp. 1487-1504, 2011.

[24] B. J. Debusschere, H. N. Najm, P. P. Lébay, O. M. Knio, R. G. Ghanem, and O. P. Le Maître, "Numerical challenges in the use of polynomial chaos representations for stochastic process," *Siam J. Sci. Comput.*,vol. 26, pp. 698-719, 2004.

[25] M. S. Eldred, C. G. Webster, and P. Constantine, Evaluation of non-intrusive approaches for Wiener-Askey generalized polynomial chaos, in *Proc. 10th AIAA Nondeterministic Approaches Conf.*, Schaumburg, IL, USA, 2008

[26] M. T. Reagan, H. N. Najm, B. J. Debusschere, O. P. Le Maître, O.M. Knio, and R. G. Ghanem,

"Spectral stochastic uncertainty quantification in chemical systems," *Combust. Theor. Model.*, vol. 8, pp. 607-632, 2004.

[27]   C. Canuto, M. Y. Hussaini, A. Quarteroni, and T. A. Zang, *Spectral Methods in Fluid Dynamics*. Springer-Verlag, New York, 1988.

[28]   H. N. Najm, "Uncertainty quantification and polynomial chaos techniques in computational fluid dynamics,"*Annu. Rev. Fluid. Mech.*, vol. 41. pp. 35-52, 2009.

[29]   D. Xiu and J. S. Hesthaven, "High-order collocation methods for differential equations with random inputs," *SIAM J. Sci. Comput.*, vol. 27, pp. 1118-1139, 2005.

[30]   Y. M. Marzouk, H. N. Najm, and L. A. Rahn, "Stochastic spectral methods for efficient Bayesian solution of inverse problems", *J. Comput. Phys.*, vol. 224, pp. 560-586, 2007.

[31]   D. Xiu, *Numerical Methods for Stochastic Computations*. Princeton, New Jersey, 2010.

[32]   F. Zhao, Z. Tian and Y. Zeng, "A stochastic collocation approach for efficient integrated gear health prognosis," *Mechan. Syst. Signal Process.*, vol. 39, pp. 372-387, 2013.

[33]   Y. Marzouk and D. Xiu, "A stochastic collocation approach to Bayesian inference in inverse problem," *Commun. Comput. Phys.*, vol. 6, no. 4, pp. 826-847, 2009.

[34]   T. L. Anderson, Fracture Mechanics: Fundamentals and Applications, 3rd ed, Taylor & Francis, 2005.

[35]   J. E. Collipriest, "An experimentalist's view of the surface flaw problem," *The Surface Crack: Phys. Problems Comput. Solutions, Amer. Soc. Mechan. Eng.*, pp. 43-61, 1972.

[36]   K. Inoue, M. Kato, G. Deng, and N. Takatsu, "Fracture mechanics based of strength of carburized gear teeth," in *Proc. JSME Int. Conf. on Motion and Power Transmissions*, Hiroshima, Japan, 1999.

[37]   O. E. Wheeler, "Spectrum loading and crack growth", *J. Basic Engng, Trans ASME*, vol. 94, pp. 181-186, 1972.

[38]   K. Ortiz and A. S. Kiremidjian, "Stochastic modeling of fatigue crack growth," *Eng. Fract. Mech.*, vol. 29, pp. 317-334, 1988.

[39]   D. A. Virkler, B. M. Hillberry, and P. K. Goel, "The statistical nature of fatigue crack propagation," Air force dynamics laboratory, AFFDL-TR-43-78, 1978.

[40]   ASTM E647-00 *Standard Test Method for Measurement of Fatigue Crack Growth Rates*. ASTM International. 2000.

[41]   D. Xiu, "Efficient collocational approach for parametric uncertainty analysis," *Commun. Comput. Phys.*, vol. 2, pp. 293-309, 2007.

[42]   C. Soize and R. Ghanem, "Physical systems with random uncertainties: chaos representations with arbitrary probability measure," *SIAM J. Sci. Comput.*, vol. 26, pp. 395-410, 2004.

[43]   S. Smolyak, "Quadrature and interpolation formulas for tensor products of certain classes of functions," *Soviet Math. Dokl.*, vol. 4, pp. 240-243, 1963.

[44]   F. Zhao, Z. Tian and Y. Zeng, "Uncertainty quantification in gear remaining useful life prediction through an integrated prognostics method," *IEEE Trans. Reliab.*, vol. 62, no. 1, pp. 146-159, 2013.

[45] C. Annis, "Probabilistic life prediction isn't as easy as it looks," *Probabilistic Aspects of Life Prediction*, ASTM STP-1450, W. S. Johnson and B. M. Hillberry, Eds., ASTM International, West Conshohocken, PA, 2003.

[46] O. Ditlevsen, R. Olesen, "Statistical analysis of the Virkler data on fatigue crack growth," *Engineering Fracture Mechanics*, vol. 25, no. 2, pp. 177-195, 1986.

[47] Z. A. Kotulski, "On efficiency of identification of a stochastic crack propagation model based on Virkler experimental data," *Archives of Mechanics*, vol. 50, no. 5, pp. 829-847, 1998.

[48] J. C. Butcher, Numerical Methods for Ordinary Differential Equations, 2nd Ed., Wiley, 2008

Fuqiong Zhao is currently a Ph.D. candidate in the Department of Mechanical Engineering, University of Alberta, Canada. She received her M.S. degree in 2009, and B.S. degree in 2006, both from the School of Mathematics and System Sciences, Shandong University, China. Her research is focused on integrated prognostics, uncertainty quantification, finite element modeling, and condition monitoring.

Zhigang Tian is currently an Associate Professor in the Department of Mechanical Engineering, University of Alberta, Canada. He received his B.S. degree in 2000, and M.S. degree in 2003, both in Mechanical Engineering, at Dalian University of Technology, China; and his Ph.D. degree in 2007 in Mechanical Engineering at the University of Alberta. His research is focused on prognostics, condition based maintenance, reliability, renewable energy systems, finite element modeling, and optimization.

Eric Bechhoefer is currently the president of Green Power Monitoring Systems, LLC. Prior to joining NRG Systems in 2010, Dr. Bechhoefer worked for the Goodrich Corporation. Dr. Bechhoefer holds 17 patents, and has authored over 70 juried papers related to condition monitoring of rotating equipment. He holds a Ph.D. in general engineering from Kennedy Western University, a master's degree in operations research from the Naval Postgraduate School, and a bachelor's degree from the University of Michigan.

Yong Zeng is a Professor in the Concordia Institute for Information Systems Engineering at Concordia University, Montreal, Canada. He is the Canada Research Chair in Design Science (2004–2014). He received his B.Eng. degree from the Institute of Logistical Engineering in 1986; and M.Sc., and Ph.D. degrees from Dalian University of Technology in 1989, and 1992, respectively. He received his second Ph.D. degree from the University of Calgary in 2001. His research is focused on the modeling and computer support of creative design activities.